Journal Pre-proofs

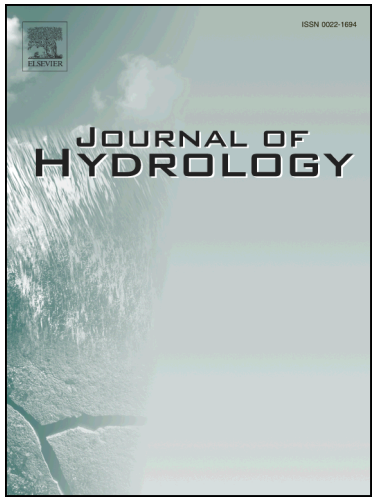

Research papers

Hydrogeological processes and near shore spatial variability of radium and radon isotopes for the characterization of submarine groundwater discharge

Carlos Duque, Karen L. Knee, Christopher J. Russoniello, Mahmoud Sherif, Usama A. Abu Risha, Neil C. Sturchio, Holly A. Michael

PII: S0022-1694(19)30927-8
DOI: https://doi.org/10.1016/j.jhydrol.2019.124192
Reference: HYDROL 124192

To appear in: *Journal of Hydrology*

Received Date: 24 April 2019
Revised Date: 23 September 2019
Accepted Date: 27 September 2019

Please cite this article as: Duque, C., Knee, K.L., Russoniello, C.J., Sherif, M., Risha, A.A., Sturchio, N.C., Michael, H.A., Hydrogeological processes and near shore spatial variability of radium and radon isotopes for the characterization of submarine groundwater discharge, *Journal of Hydrology* (2019), doi: https://doi.org/10.1016/j.jhydrol.2019.124192

Hydrogeological processes and near shore spatial variability of radium and radon isotopes for the characterization of submarine groundwater discharge

Carlos Duque[1, 2], Karen L. Knee[3], Christopher J. Russoniello[2,4], Mahmoud Sherif[2,5], Usama A. Abu Risha[6], Neil C. Sturchio[2] and Holly A. Michael[2,7]

[1]WATEC, Department of Geoscience, Aarhus University. Aarhus, Denmark
[2]Department of Geological Sciences, University of Delaware. Newark, DE, USA
[3]Department of Environmental Science, American University. Washington, DC, USA
[4]Department of Geology and Geography, West Virginia University, Morgantown, WV, USA
[5]Department of Geology, Tanta University, Tanta, Egypt
[6]Geology Department, Desert Research Center. Cairo, Egypt
[7]Department of Civil and Environmental Engineering, University of Delaware. Newark, DE, USA

Abstract

Inadequate characterization of variability in natural tracers of submarine groundwater discharge (SGD) introduces large errors into tracer-derived SGD estimates. To address this gap, we investigated spatial variability in the natural SGD tracers ^{223}Ra, ^{224}Ra, ^{226}Ra, ^{228}Ra and ^{222}Rn using a high-density array of piezometers and seepage meters over a nearshore area where discharging groundwater transitioned from fresh to saline. Seepage meters and piezometers were used to sample groundwater and to quantify fluxes and salinity. A series of spatial patterns was distinguished beyond the normal salinity impact on Ra activity. The discharge in the interface between saltwater and freshwater was characterized by higher activities of the longer-lived isotopes (^{226}Ra and ^{228}Ra), while areas dominated by benthic exchange had higher activities of the shorter-lived isotopes (^{223}Ra and ^{224}Ra). Spatial differences in Ra activities were associated with variation in salinity and residence time in the aquifer and were indicative of underlying hydrogeological processes. At the freshwater-saltwater interface, fresh discharge is driven by terrestrial hydraulic gradients and saline discharge is driven by density gradients; both result in long residence times in the aquifer. Benthic exchange of saltwater has shorter residence times, much less than required to enrich long-lived isotopes and reach secular equilibrium. The highest activities of ^{222}Rn were detected in the fresh discharge zone, and the lowest activities in areas

dominated by benthic exchange. Direct sampling at discharge points allowed comparison between groundwater collected from inland wells and the water discharging to the bay, and indicated significant differences in the activities despite the short distance from wells to the discharge area. Substantial spatial variability in Ra and Rn was observed on the meter scale, with trends that reflected groundwater origin and residence time. Inadequate characterization of variability, trends, and fluxes introduces large errors into tracer-derived estimates of submarine groundwater discharge. Thus, the study of submarine groundwater discharge with radioactive tracers requires adequate hydrogeological knowledge to identify processes that have strong impacts on Ra and Rn activities and associated fluxes to the ocean.

Introduction

The use of naturally occurring radioactive tracers for quantifying submarine groundwater discharge (SGD) has become a standard method within the scientific community over the last two decades since its first use (Moore, 1996). These tracers have been applied in coastal locations around the world. Notable improvements in analytical techniques (e.g., Moore, 2008; Molina Porras et al., 2017) have been made, and our understanding of the processes that must be considered when using a mass balance based on radioactive tracers continues to improve. Quantification of groundwater discharge is required for investigation of ocean budgets of constituents such as silica (Tréguer and De La Rocha, 2013), calcium carbonate (Milliman, 1993), and excess nutrients (Kelly and Moran, 2002; Krest et al., 2000; Rapaglia et al., 2010; Sadat-Noori et al., 2016) that are usually associated with anthropogenic sources such as fertilizers and wastewater. Nutrient and other SGD-borne pollution inputs can severely impair coastal ecosystems (Johannes, 1980; Valiela et al., 1990). However, SGD can be one of the most challenging terms

in the water budget to quantify. SGD is usually not visible and occurs under the sea, so indirect methods are required to detect and measure it. SGD can be especially important on oceanic islands (e.g. Kim et al. 2011, Knee et al. 2016) and in arid coastal environments where freshwater resources are scarce (Gallardo, 2019) and groundwater is essential for water management (Duque et al., 2018; Eissa et al., 2018).

The most common natural tracers used for estimating water budgets in coastal areas are ^{223}Ra, ^{224}Ra, ^{226}Ra, ^{228}Ra and ^{222}Rn. The four Ra isotopes are generated from the disintegration chains of U and Th present in rocks and sediment grains, and therefore they are generally more abundant in groundwater relative to seawater (Rama and Moore, 1996) or meteoric freshwater. Ra decays but otherwise generally behaves conservatively once released into marine and surface waters (Charette et al., 2001). ^{222}Rn is the daughter of ^{226}Ra. As a noble gas, it does not react with sediments or water when transported in groundwater, but it can evade to the atmosphere (Ellins et al., 1990). Properties that make Ra and Rn effective tracers include their natural origin, reliability of measurements and the potential to integrate processes that can be highly heterogeneous (Burnett et al., 2006; Stieglitz et al., 2008).

The usual natural tracer methodology consists of a mass balance defining the sources and sinks for the surface water body that is being studied (Burnett et al., 2010; Cable et al., 1996). Ra sources and sinks include generation by alpha-recoil and desorption from benthic or suspended sediments, radioactive decay, adsorption or co-precipitation, mixing with other waters with different compositions (for example in bays with the ocean water), river inputs, and SGD. Generally, the sources and sinks other than SGD are calculated based on assumptions or data, and the input of the tracer from SGD is then estimated by difference. In order to calculate the SGD flux, the tracer concentration in discharge must be known, this is termed the *endmember*. Endmembers may

include one or more types of discharging groundwater, open ocean water, and/or river water. Finally, the residence time of water in the receiving water body is estimated either using Ra-based or other methods and used to calculate the water input from SGD (Cable et al., 1996; Corbett et al., 1999; Ellins et al., 1990; Rama and Moore, 1996).

Accurately estimating the groundwater endmember Ra or Rn concentration is critical for obtaining an accurate SGD calculation, but it can be difficult to accomplish. In a review of 116 studies in different world locations, Girault et al. (2016) showed 9 and 6 orders of magnitude variation in the activities of samples for ^{222}Rn and ^{226}Ra, respectively. Similar results were found by Dragović et al. (2012) related to the geological and environmental conditions of samples in Serbia for ^{226}Ra and by Zhuo et al. (2001) whose inventory of 552 groundwater samples in southwest China showed several orders of magnitude variability in ^{222}Rn activity. At local scales, substantial heterogeneity has also been observed (Gonneea et al., 2008; Sadat-Noori et al., 2015; Stachelhaus et al., 2012). This variability has been highlighted as one of the main challenges in defining the groundwater endmember (Krest and Harvey, 2003; Michael et al., 2011) and the main source of uncertainty both for Rn (Atkins et al., 2013; Dimova et al., 2013; Peterson et al., 2010) and Ra (Hughes et al., 2015; Kim et al., 2005) tracer methods.

There are several causes for the Ra and Rn variability in groundwater. One is a difference in generation rates due to heterogeneity in sediment composition (Burnett and Dulaiova, 2003; Michael et al., 2011). This has been shown through lab experiments using sediment cores (Gonneea et al., 2008), where layers $\leq$ 1 m apart interacted differently with water. Salinity is another factor that substantially affects sorption-desorption processes for Ra (Rama and Moore, 1996; Swarzenski, 2007). In coastal areas, salinity plays a key role since freshwater transitions to saltwater in both surface water and groundwater, often over short distances. Other geochemical

variations can also affect Ra behavior, such as pH (Lauria et al., 2004; Sanchez and Rodriguez-Alvarez, 1999), redox conditions (Sturchio et al., 2001; Vinson et al., 2009), and major dissolved ions (Onishchenko et al., 2010).

The difficulty in defining the groundwater endmember is also a problem of scale. Because activities differ over short distances, a few meters or less (Schmidt et al., 2009; Smith et al., 2008), using the mean value of a few isolated samples can be unreliable. Several studies address the problem of the required number of samples for decreasing uncertainties in the definition of the groundwater endmembers (Charette, 2007; Makings et al., 2014; Santos et al., 2014). Sadat-Noori et al. (2015) tested how results varied with an increasing number of Rn samples (n=27) in groundwater. In their study area, they found that 20 samples adequately represented the average regional Rn activity.

Another issue is that the activity of natural tracers in coastal discharging groundwater often does not just have a unimodal distribution with a high variance; rather, it is a multimodal distribution because it is composed of varying proportions of groundwater types with different origins and chemistries. Three primary mechanisms drive groundwater discharge in coastal areas: discharge of freshwater from inland recharge (Fig. 1. Flow 1), convective saltwater circulation driven by density gradients (Fig. 1. Flow 2), and small-scale saltwater circulation, or benthic exchange, due to processes such as tides, waves and currents (e.g., Russoniello et al., 2018; Santos et al., 2012; Sawyer et al., 2013) (Fig. 1. Flow 3). In the case of Ra, average activities, even considering overall variability, are generally significantly different among groundwater of different origin (e.g., Liu et al., 2018; Michael et al., 2011). Ra activities are often very low and similar to surface water in fresh groundwater (making the tracer useless for this portion of SGD), highest in brackish groundwater, and intermediate in saline groundwater. Thus, in order to define a single endmember,

it would be necessary to define the tracer concentration in each type of groundwater and determine the proportion of flux contributed by each.

Figure 1

Despite all of these complications and the importance of knowing the endmember value, it is common in the literature to find the definition of endmembers based on between a few and a dozen samples, generally due to practical limitations such as the availability of wells or the possibility of obtaining a large enough sample (i.e. Garcia-Solsona et al., 2008). Additionally, relevant geochemical data such as salinity is often missing. In most cases, authors do not discuss how representative the groundwater samples are from a hydrogeological perspective. For example, Cho and Kim (2016) indicated the possibility of a global overestimation of SGD rates due to the frequent use of endmembers with lower salinity that would transport a lower amount of Ra, possibly because inland wells are generally drilled to obtain freshwater and not saltwater (Michael et al., 2011). Further, Ra activities in sampled inland groundwater may be quite different than in discharging groundwater due to geochemical alteration along flowpaths. The definition of the groundwater Ra and Rn endmember has a critical impact on the results obtained, but this aspect of the research is often minimized compared with the typically more thorough characterization of the Ra and Rn distributions in surface water.

Even with the wide application of these tracer methods and the difficulty in endmember estimation, few studies have systematically measured discharging groundwater discharge directly to characterize the spatial variability of radioactive tracer activities. Studies with higher spatial resolution have been limited to cross sections (i.e. Dimova et al., 2013; Dulaiova et al., 2008; Liu et al., 2018; Michael et al., 2011) that consider onshore-to-offshore variability related to flowpaths, salinity, or water origin, but cannot capture aquifer heterogeneity that results in small-scale and

alongshore variations. In this work we characterize tracer activities in discharging water using seepage meters and piezometers arranged in a dense, 2D grid to understand meter-scale variability in Ra and Rn activities and fluxes. The measured activities of ^{223}Ra, ^{224}Ra, ^{226}Ra, and ^{228}Ra and ^{222}Rn were compared with measured SGD fluxes and salinity and knowledge of the associated flow system to investigate the association between hydrogeological processes and radioactive tracer distributions. This understanding is essential to improve the application of these widely-used tracer methods and to obtain more accurate estimates of SGD and associated chemical fluxes to oceans and surface water bodies.

Study area

Two field campaigns were conducted at Holts Landing State Park (Delaware, USA) on the southern shore of Indian River Bay (Figure 2), a 37 km^2, shallow (~3 m maximum depth), microtidal (mean tide range 0.82 m) estuary on Delaware's Atlantic coast. Topography in the 223 km^2 watershed is subdued with a maximum elevation of 16.5 m (Russoniello et al., 2016). A mean annual precipitation of 1140 mm is distributed throughout the year. Air temperature varies considerably between summer (mean = 25 ^{o}C) and winter (mean = 2 ^{o}C) (NOAA/NCDC, 2010) resulting in variable recharge due to changes in evapotranspiration rates that drive annual water table fluctuations of several meters (Andres et al., 2015). The ecological health of the watershed has declined in recent decades as high nutrient loads from development and agricultural practices have caused eutrophication (Bratton et al., 2004). High hydraulic conductivity of shallow sediments throughout the watershed results a significant seaward nutrient transport via groundwater (e.g. Andres, 1992; Russoniello et al., 2016).

The geology of the area is dominated by a thick series of sedimentary units (2500 m) which are topped by the Pleistocene Beaverdam Formation (*Fm.*) (Ramsey, 2010). In many places the silty

sands of the Beaverdam Fm. have been eroded and infilled with Holocene estuarine peats and clays (Chrzastowski, 1986; Krantz et al., 2004; Russoniello et al., 2013). These paleovalley fill sequences act as low-hydraulic conductivity (K) caps that prevent nearshore SGD, whereas in interfluve areas without clay caps, the discharge is more focused along the shoreline (e.g. (Bratton et al., 2004; Russoniello et al., 2013; Sawyer et al., 2014). In Holts Landing State Park, a series of breakwaters was constructed meters away from the shore to prevent erosion of the coastline. This has created a fringe where the deposition of fine sediments has been enhanced, especially during low tide, generating another cap layer (Figure 2) along the shoreline with low hydraulic conductivity that prevents the discharge of groundwater close to the shore and causes groundwater to discharge on the other side of the breakwater. The intertidal circulation of saltwater due to tide and wave action observed at other locations (e.g. Heiss and Michael, 2014; Michael et al., 2005; Robinson et al., 2007; Xin et al., 2010), is absent at this field site because of the breakwater and the low-K fringe. This situation is fortuitous for the measurement of SGD because the relatively deep (~1m) and flat area of bayfloor with soft sediments and low wave action is an ideal location for the installation of seepage meters. In most coastal areas, no cap layer exists near the shore, so SGD occurs right at the shoreline, where variable water depth, wave action, and a steeper slope make the use of seepage meters more difficult in the proximity of the shore line.

We selected a study area in the interfluve with relatively homogenous hydrogeology unaffected by the presence of paleochannels, so only the effect of intra-unit heterogeneity within the Beaverdam Fm. was considered. This information was provided by previous studies using geophysics and seepage meters (Krantz et al., 2004; Russoniello et al., 2013). The location of the seepage meter grid was aligned with the flow direction from one of the wells inland (Well 4) (Fig. 2), and it was also in close proximity to the other wells (Fig. 2). This facilitated comparisons

between the chemistry of inland groundwater and discharging groundwater collected from seepage meters.

Figure 2

Methods

Two field sampling campaigns were conducted - a preliminary survey on October 26-30, 2015 and a complete survey on July 13-17, 2016 to measure spatial variations in SGD rates and chemistry. Submarine groundwater discharge measurements were made with 30 Lee-type seepage meters (Lee, 1977) constructed from steel 55-gallon drums with a diameter of 58 cm, following the recommendations of previous studies (Michael et al., 2003; Russoniello and Michael, 2015). Detailed descriptions and images of the design and function of these seepage meters are presented elsewhere (i.e. Duque et al., 2018; Rosenberry, 2005). Seepage meters were painted on all sides to prevent corrosion.

Seepage meters were deployed in a rectangular grid with 5 rows (cross-shore direction) and 6 columns (along shore direction) with approximately 3 m spacing in both campaigns (Figure 2). Seepage meter locations were based on knowledge of SGD patterns at the field site (Russoniello et al., 2013; Sawyer et al., 2014) and were measured with a Trimble RTK GPS with centimeter horizontal precision. Seepage meters were deployed for the second campaign in approximately the same location as the first campaign. In both instances, seepage meters were installed several days prior to commencement of the campaign to allow discharging groundwater to flush the seepage meter headspace before measurements were made. Electrical conductivity, temperature and depth

sensors (*CTD*; In Situ Aquatroll 100) were deployed in three seepage meters to verify that groundwater fully flushed the seepage meter headspace by the commencement of the campaign.

Seepage meter samples were collected in thin-walled, durable plastic autoclave bags. During the first campaign in October 2015, the bags were prefilled with 2 L of Ra-free tap water to allow measurement of groundwater recharge and to prevent bag-induced measurement artifacts (e.g. Murdoch and Kelly, 2003; Shaw and Prepas, 1989). During the July 2016 campaign, the bags were attached empty because high discharge and zero recharge had been observed in the previous campaign and bag-induced flow measurement artifacts were considered minor compared with the potential influence on salinity and tracer concentrations, considering the overall high discharge rates. During the October 2015 campaign, seepage meters were sampled three times over a half-tidal cycle at 2-h intervals (10:00-12:00, 12:00-14:00, 14:00-16:00). During the July 2016 campaign, each seepage meter was sampled five times over a half tidal cycle (9:00-11:00, 11:00-13:00, 13:00-15:00, 15:00-17:00, 17:00-19:00). After each interval the sample bag was removed and a previously prepared bag was immediately affixed to prevent inflow of bay water to the seepage meter during the bag exchange. Each bag had a valve so that it could be closed during removal and while unattached. This bag exchange was completed by 3-5 operators to obtain an approximately simultaneous sampling of all the seepage meters. The total time for sample collection and bag replacement never exceeded 30 minutes. Electrical conductivity (EC) corrected to 25 ^{o}C of seepage meter samples, groundwater and surface water samples was measured by using a YSI EC300 handheld conductivity instrument (expected error less than 1% of the reading). For seawater at a given temperature, EC and salinity are directly proportional to each other, and for ease of comparison with other studies we present the equivalent salinity value for key EC measurements. The percentage of freshwater and saltwater flux for each discharge sample was

calculated by assuming an electrical conductivity of 0.7 mS/cm (salinity < 1 g/L) for the fresh water endmember based on the EC of the well closest to the discharge area and conductivity for the saline endmember equal to that measured for bay water on the day of sampling (range 41-47mS/cm or 26.2-30.5 g/L).

Discharge accumulated in each seepage meter was retained for Ra analysis. Differing SGD rates to each seepage meter resulted in different water volumes collected for Ra analysis. Sample volumes ranged from 6.5-17 L in October 2015 and from 9-83 L in July 2016. In October 2015, 19-L buckets were used to transport samples back to the lab for analysis, necessitating a fraction of large-volume samples to be discarded; however, in July 2016 the entire collected volume of each sample was processed on-site.

Rn sampling was done by extracting groundwater with a PushPoint minipiezometer (diameter 5 mm and screen of 3 cm) (M.H.E. Products, East Tawas, MI) at 25 cm depth during sample collection. The insertion process did not allow groundwater into the piezometer until the screen was located at the correct depth, but a 50-100 mL volume (2.5-5 times the volume in the sampler for a 25-cm water column) was discarded before the sample was collected to guarantee a representative sample of groundwater. Extraction was accomplished by slow suction with a tube attached to a syringe, keeping the sample at constant extraction pressure to prevent degassing or mixing with atmospheric air. Samples were collected in 250-mL gas-tight bottles, which were filled from bottom to top and overflowed prior to capping to prevent degassing and atmospheric exchange. If bubbles were generated during sampling, the sample was discarded and a new, bubble-free sample was collected. Samples were analyzed within four days (and generally within less than 24 hours) using a RAD7 radon detector with RAD H2O accessory (Durridge Co., Billerica, MA). The WAT250 measurement protocol was used, except that counting time was

extended from the default of 30 minutes to 3 hours per sample to reduce uncertainty resulting from low sample activity.

For analysis of Ra isotopes, Ra was pre-concentrated by adsorption from each water sample onto Mn-oxide coated acrylic fiber (Dulaiova and Burnett, 2004; Kim et al., 2001; Moore and Reid, 1973). Water was aerated before Ra adsorption to cause degassing and oxidation that would help ensure quantitative extraction (Dulaiova and Burnett, 2004). Turbidity was negligible and water was not filtered. Water was passed slowly (< 1 L per minute) by gravity feed through ¼-inch plastic tubing into the inlet of a 100 cm^3 flow-through cartridge containing 14 g of Mn-coated acrylic fiber (Scientific Computer Instruments, Columbia, SC), which adsorbed Ra from the water. After draining and removal from the cartridge, the fiber was transferred to a labeled plastic Zip-loc bag for transport to the laboratory. Extraction efficiency was evaluated by passing water through two columns in series, and no detectable Ra was found in the downstream column, indicating essentially quantitative removal by the first column.

For short-lived isotope (^{223}Ra and ^{224}Ra) analysis, Mn fibers were rinsed with fresh tap water and air-dried to achieve a water to fiber weight ratio of between 0.4 and 1.1 for optimum counting efficiency (Moore, 2008; Sun and Torgersen, 1998). Short-lived Ra isotope activities were then measured on a Radium Delayed Coincidence Counter (RaDeCC) system at American University using the protocols described by Knee et al. (2008) and Street et al.(2008), based on techniques developed by Moore (1976) and Moore and Arnold (1996). Initial ^{223}Ra and ^{224}Ra measurements were made within 10 days of collection, and all samples were run a second time 3-6 weeks after collection to correct for ^{228}Th- supported ^{224}Ra activity. The error associated with each short-lived Ra isotope measurement was calculated using methods described by Garcia-Solsona et al. (2008). Median relative errors were 37% and 18% of sample activity for ^{223}Ra and ^{224}Ra respectively, and

any measurements with relative errors >100% (corresponding to low activities close to the lower limit of detection; n=3 for ^{223}Ra and n=1 for ^{224}Ra, respectively) were considered to have an activity of half the lower limit of detection. This lower limit was estimated as 0.1 dpm/100 L for ^{223}Ra and 1 dpm/100 L for ^{224}Ra. The estimate for the lower limit of detection was based on the uncertainty, which is itself a function of the number of decays counted over the maximum 4-h run time and the background counts per minute recorded by the RaDeCC system. As the number of counts decreases, the relative uncertainty increases and approaches 100%, which is interpreted as the lower detection limit. The number of counts is influenced by the sample activity as well as the sample volume and the time elapsed between collecting and running the sample. In this case, we inspected the calculated activity and relative uncertainty of each sample, estimated the activity when relative uncertainty was equal to 100%, and assumed that to be the lower detection limit.

For ^{226}Ra and ^{228}Ra, the Mn-fiber samples were ashed at 700 °C and sealed after cooling in labeled 7-mL polypropylene vials. Two high-purity Ge gamma spectrometers (Model GWL-170-15-LB-AWT with 15 mm well diameter, EG&G Ortec, Ametek, Inc.) were used to measure sample gamma emissions at the University of Delaware. ^{226}Ra was measured from its emission at 186.2 keV, and ^{228}Ra through the ^{228}Ac gamma emission at 911.3 keV. Reference measurements were calibrated with certified NIST-4965 and NIST-4339b Standard Radium Solutions (US National Institute of Standards and Technology). Specific activities and one sigma errors were calculated using standard counting techniques (Mook, 2001) and are reported in units of becquerels per kilogram (Bq/kg) and converted to dpm/100 L. Activities were corrected for detector background and for decay that occurred between sample collection and analysis on the gamma spectrometer. The limit of detection for each radionuclide was defined as three times the standard deviation of

the background under the peak used for the activity quantification. Reported analytical errors are ±1 standard deviation based on counting statistics.

Five nearby onshore wells were sampled to estimate Ra and Rn activities in the groundwater endmember(s) as it is usual in SGD studies. Wells were purged by pumping three times the volume stored in the well prior to each sampling. These wells had different salinities due to the intersection of the saltwater-freshwater interface at different depths. A CTD logger was installed in a well located 70 m inland of the shoreline to record changes in the water table elevation and EC at 10 to 15 minute intervals. A CTD was also installed beneath a nearby pier to record the tide level of bay water. A barometer installed at the well allowed for atmospheric corrections to be made to measurements from both sensors.

Groundwater below the area covered by the seepage meters along a transect was collected with samplers every 25 cm up to 1.5 m depth. EC was measured to establish how freshwater transitions to saltwater in the aquifer below the bay and verify the results obtained with the seepage meters.

Here, we present results from the July 2016 sampling campaign because it was more complete (for 2015 only 10 samples were collected for ^{222}Rn), the analytical methods were corrected and adapted to the characteristics of this zone (analytical uncertainties were reduced by increasing sample volumes and/or increasing the counting time), and the field methods were tested and improved after the 2015 reconnaissance survey (a system for Ra extraction of samples in situ was constructed and two RAD7s were used for in-situ analysis of ^{222}Rn). In spite of the improvements in the methodologies, it was possible to detect that the general trends observed in 2015 were similar in 2016 indicating that the results presented here are consistent during longer periods of time and not only applicable to the specific time of sampling.

Results

Salinity and flux distribution

The samples collected from the seepage meter bags and from direct sampling with the PushPoint sampler in the aquifer adjacent to each seepage meter showed a salinity distribution that reflected the location of the freshwater-saltwater interface. The seepage meter grid spanned an area where freshwater was dominant, another where saltwater was dominant, and the transition or interface zone between them. The measured EC ranged from fresh (< 2 mS/cm, salinity < 1 g/L) to saline (> 40 mS/cm, salinity >25.5 g/L) over a distance of less than 6 m. The interface zone was ~3-5 m wide (Figure 3A). The sampling locations were classified as freshwater-, saltwater-, or interface-dominated based on the salinities measured and the spatial distribution. The first two rows (12 sampling points) were classified as freshwater, 7 points as freshwater-saltwater interface, and 11 points, located mostly in the last two rows were classified as saltwater. Two or three points classified as interface could also have been classified as saltwater (Fig 3C). The flux distribution varied somewhat with salinity. In general, higher fluxes were measured in the freshwater and interface areas (Table 1) compared to the saltwater area further offshore (Fig. 3B). The highest fluxes were associated with the saltwater-freshwater interface (Fig 3C). Similar distributions have been observed in other studies at different sites (Duque et al., 2018; Michael et al., 2005)

Figure 3

Tracer results

Rn and Ra activities (Duque et al., 2019) were characterized for each zone with descriptive statistics (Tables 1 and 2). The mean analytical error compared with the mean value was highest for ^{226}Ra (41%) and lower for the other Ra isotopes (^{223}Ra-36%, ^{224}Ra-25% and ^{228}Ra-3%) (Table

2). Measurements were highly variable, ranging from below detection limit to high values, due to the different environments (variations in salinity, flow paths, fluxes) that were captured in the samples (Tables 1 and 2).

Table 1

Ra activity varied strongly between categories, with much lower values in fresher discharge (Table 2). In the interface zone, groundwater fluxes, activities and standard deviations of ^{226}Ra and ^{228}Ra were greatest. ^{222}Rn activities were highest in fresh discharge and lowest in the saltwater zone (Table 1). While ^{222}Rn activities are not affected by salinity, differences between freshwater zone and saltwater zone were observed.

Table 2

Table 3

Differences in Rn and Ra activity among the salinity categories were evaluated (Figure 4; Table S1) using a two-sample Student's *t*-test were completed by testing the null hypothesis that the means each pair of categories (saltwater-freshwater, saltwater-interface, interface-freshwater) were the same. If the null hypothesis was rejected, the interpretation is that the two categories had significantly different mean values. The *t*-test is a standard and widely used statistical method.

For ^{223}Ra, ^{224}Ra, and ^{228}Ra, saltwater activity was significantly higher, 3-4 times higher than that of freshwater. The minimum values, near the lower detection limit, were all located in the freshwater zone. For ^{223}Ra and ^{224}Ra, freshwater and saltwater were significantly different (SW-FW: ^{223}Ra p $=2.6\cdot10^{-3}$, ^{224}Ra p $=1.7\cdot10^{-4}$), while the interface was not statistically distinct from the saltwater zone (SW-INT: ^{223}Ra p $=4.2\cdot10^{-1}$, ^{224}Ra p $=4.4\cdot10^{-1}$). For ^{226}Ra and ^{228}Ra, the distinction between saltwater and freshwater is clear (SW-FW: ^{226}Ra p-value $=9.2\cdot10^{-2}$, ^{224}Ra p $=1.2\cdot10^{-9}$). The

t-test could not statistically differentiate between saltwater and interface zones (SW-INT: ^{226}Ra p =1.9·10^{-1}, ^{228}Ra p =3.5·10^{-1}), probably due to the high variability of concentrations in the interface zone (Fig. 4).

^{222}Rn activity showed a gradual transition from the location where freshwater was dominant (high values) to the saltwater areas (low values), and a t-test confirmed that freshwater (n=12) had significantly higher ^{222}Rn than saltwater (n=11) (p = 1.2·10^{-3}).

Figure 4

Rn and Ra activities in inland wells varied over a large range. Although they are located at variable distances from the shore (Figure 1) and at different depths, they are all within 120 m of the seepage meter grid and in the same geological unit. Wells 1, 2, and 3 are nested at different depths in the same location, and the screens intersect different parts of the salinity interface (detailed information about the wells and their characteristics can be found in Andres et al., 2015); thus differences in Ra (Table 3) are related to the depth and salinity. Well 4 is closest to the location of the seepage meter grid and probably in the same flow line of groundwater discharging to the bay (Figure 1), hence it was selected to compare groundwater in wells with that discharging to the bay.

Spatial distribution

Ra activities generally increased from the fresh to saline portions of the sampling grid, which is expected due higher mobility of Ra with higher salinity (Elsinger and Moore, 1984). However, within salinity zones, there was strong spatial variability in Ra over short distances (Figure 5). The lowest Ra activities generally occurred in the row of seepage meters located closest to the shoreline where there was the greatest proportion of freshwater, but the highest activities did not occur in the most offshore row for all the Ra isotopes. In the case of long-lived isotopes ^{228}Ra and ^{226}Ra,

the maxima were located in the freshwater-saltwater interface zone, but activities were highly variable. For the short-lived isotopes ^{223}Ra and ^{224}Ra there was a more gradual transition from the freshwater sampling points, where activities were near 0, to the maximum values located in the saltwater area (Figure 5).

Figure 5

Comparison between ^{228}Ra and ^{222}Rn with respect to electrical conductivity shows the differences between the tracers (Figure 6). The highest activity of ^{222}Rn was located in the freshwater zone, closest to shore. It was much lower, near the lower detection limit, in the saltwater zone. ^{222}Rn activity decreased systematically with salinity, unlike Ra, which peaked at intermediate salinity. There was also spatial variability in the activities measured for each of the salinity zones defined. The activity of ^{222}Rn for samples collected in the freshwater area ranged from 25-200 pCi/L and from 0-100 pCi/L for samples collected in the saltwater area. ^{228}Ra activities ranged from 0 - 50 dpm/100L for freshwater samples and 50 – 300 dpm/100L for saltwater samples (Fig. 6).

Figure 6

Discussion

Spatial variability of Ra and Rn

These results illustrate the meter-scale spatial variability of natural SGD tracer activities. The sampling points were located 3 meters apart and the maximum distance within the study area was less than 20 m. Nevertheless, the observed activities varied by up to a factor of 1000, even for this small area. A key controlling factor was salinity or groundwater origin, as the variability in activity is reduced when samples of ^{222}Rn and Ra are compared only within areas dominated by freshwater

or saltwater. This observed heterogeneity complicates endmember definition in the application of these tracers to more extensive areas, for example with the utilization of isolated samples that can introduce large errors into estimations of the average activity of Ra and Rn in SGD.

The spatial variability of Ra has been observed and described previously based on cross-sectional studies (Knee et al., 2008; Liu et al., 2018; Michael et al., 2005; Street et al., 2008). However, in this case it is possible to see that there is also high lateral variability along shore. In principle, the observed differences between activities of different Ra isotopes are related to their half-lives and the abundances of their parent isotopes in the U and Th series, since the chemical behavior of the isotopes is identical. Thus, variation in water flow paths and residence times are likely to control the differential behavior of Ra isotopes in groundwater (e.g., Michael et al., 2011).

Salinity changes in groundwater and impact over radioactive tracers

The freshwater-saltwater interface will be present in any coastal area where there is freshwater discharge. Accounting for the salinity distribution when developing a sampling plan for characterizing radioisotope concentrations in endmembers will help to reduce bias and uncertainty. This is illustrated by the samples that were collected from the inland wells. Wells 1, 2, and 3 are all located the same distance from shore, but at different depths. The Ra activities for each of the wells were distinct due to the salinity changes with depth produced by the saltwater-freshwater interface location. Each of the wells would be more representative of freshwater or saltwater so an optimal approach would be to select the sample that is more representative of the desired endmember (i.e. freshwater or saltwater discharge) and to characterize its uncertainty.

The challenge in defining representative endmembers associated with salinity distributions can also be temporal. The freshwater-saltwater interface location is affected by transient processes

such as water abstraction for irrigation and supply, changes in inland recharge, and climatic oscillations. This complicates sampling in longer term studies since it cannot be assumed that endmember activities are constant (Cerdà-domènech et al., 2017). This would have a direct impact, for example, in regions with marked seasonal oscillations that could lead to an apparent higher Ra activity in the dry seasons than in the wet season if the same wells were sampled without considering movement of the saltwater-freshwater interface. Changes in the inland water table can also alter the position of the salinity discharge zones offshore, which would need to be considered for the appropriate placement of seepage meters.

A second complication in defining endmembers is the variation in activities along flowpaths. A simple comparison of the arithmetic mean of the dataset collected in the seepage meters with the measurements in Well 4, located along the flow line of the discharging water at a distance of less than 100 m, showed an enrichment from Well 4 to discharge point of: 175%, 278%, 20% and 374% of the seepage meter average for ^{223}Ra, ^{224}Ra, ^{226}Ra and ^{228}Ra, respectively. The cause for this may be differences in the water sources or geochemical processes along the flowpath prior to discharge. Since the EC in the well was similar to the discharging freshwater (EC =0.6 mS/cm or salinity <1 g/L), the same comparison can be done with only the freshwater samples in the seepage meters with these results: -75%, -73%, -25% and -69% for ^{223}Ra, ^{224}Ra, ^{226}Ra and ^{228}Ra respectively. Seepage meter samples collected in the freshwater zone were fairly similar, in terms of EC, to well water. Well 3 had the highest EC (20 mS/cm or salinity ~ 12), making it the most comparable to saline seepage meter samples. Despite having similar EC to these saline seepage meter samples (Table 2), the well had Ra activities 5-25 times higher. This may reflect saline wedge interception in the well and/or that the well and the groundwater discharge zone are along different flowpaths (the well is located around 120 m to the West of the sampling area). In general,

these comparisons indicate that groundwater samples from wells may not adequately represent SGD to the surface water body; the distance between the well and discharge point is critical and large differences can occur over short distances. For this reason, direct sampling from discharging water is recommended.

Flow paths and Ra distribution

Coastal groundwater flow and mixing processes occur on a range of time scales similar to the range in Ra half-lives, which are proportional to production rate. As a result, Ra isotope ratios can potentially be used to understand flow processes in coastal groundwater systems. ^{226}Ra and ^{228}Ra have half-lives of 1600 years and 5.8 years respectively; therefore, if they are removed by any process it will take a long time to reach a new equilibrium. The half-lives of ^{223}Ra and ^{224}Ra are much shorter (11.4 and 3.6 days, respectively) and while long-lived isotopes reflect an integrated value of the processes taking place in the system, the short-lived isotopes are more sensitive to the immediate environment (Rama and Moore, 1996). Assuming that variations in the underlying geology do not affect Ra isotope production in the study area, a relatively high ^{223}Ra/^{228}Ra or ^{224}Ra/^{228}Ra ratio would indicate the dominance of short residence time processes since short-lived isotopes respond more quickly to changes than long-lived isotopes (Rama and Moore, 1996). Previous studies with analytical simulation of the generation of Ra isotopes (Michael et al., 2011; Tamborski et al., 2017) showed that it takes ~20-30 days to fully regenerate the short-lived isotopes of Ra and much longer (years) for ^{226}Ra and ^{228}Ra. Therefore, these results would be indicative of processes that are shorter or longer than about one month (Charette, 2007; Michael et al., 2011; Moore, 2003). Here, we refer to these as "fast" and "slow" processes, respectively. Saltwater recirculation (benthic exchange) is a fast process that does not allow enough time for the longer-lived isotopes of Ra (^{226}Ra and ^{228}Ra) to build up in groundwater. A longer flow path, such as that

along the saltwater-freshwater interface driven by density gradients, would allow for generation of ^{228}Ra, and potentially ^{226}Ra (depending on the ratio of residence time to production rate) and would be considered slow.

Considering this conceptualization, ^{226}Ra and ^{228}Ra activities were highest in the interface zone between fresh and saline groundwater (Figs. 4 and 5). Two different underlying mechanisms could produce this pattern. One possibility is that the freshwater-saltwater interface moves back and forth seasonally. During wet periods, Ra would accumulate by adsorption to the surfaces of sediments in the freshwater part of the aquifer. Then, during drier periods, the saltwater-freshwater interface would retreat and saltwater would flow into this part of the aquifer, increasing the desorption of Ra and allowing it to be flushed out. The accumulation and release of Ra connected to the changes in water table and the oscillations of the saltwater-freshwater interface has been described as an explanation for the changes in Ra activity along vertical profiles (Dulaiova et al., 2008). The reasons for changes in the saltwater-freshwater interface position are connected to inland recharge, which oscillates seasonally in this temperate zone due primarily to evapotranspiration and precipitation changes (e.g., Michael et al., 2005).

A second potential reason for high long-lived isotope activities along the interface is that discharge in this zone is a result of longer groundwater flow paths with greater residence time. Density driven flow induces groundwater to follow a circulation path downward and then upwards along the freshwater-saltwater interface (Kohout, 1964). This hydrogeological process causes groundwater to circulate for a longer time in contact with the sediments, increasing the content of ^{228}Ra and potentially ^{226}Ra. The spatial distribution of Ra isotope ratios support this interpretation. The ratios of short-lived to long-lived isotopes, ^{223}Ra/^{228}Ra and ^{224}Ra/^{228}Ra, are greatest in the areas where saltwater is dominant and lower in interface areas (Figure 7). This reflects the difference in

residence time between discharge driven only by benthic exchange (short residence time), as expected in the saltwater only zone, and discharge driven by density gradients (longer residence time). A short groundwater residence time results in a higher short-lived to long-lived isotope ratio than a long residence time. The $^{228}Ra/^{226}Ra$ ratios have a more homogeneous distribution in the saltwater areas (Figure 7) since both isotopes are indicators of regional processes in the system and they are not as useful for resolving processes occurring on shorter time scales.

Figure 7

^{222}Rn

Salinity has a minor effect in the solubility of ^{222}Rn (Schubert et al., 2012). Usually it is assumed that ^{222}Rn is transported by groundwater once it is generated by decay of ^{226}Ra as a consequence of its high solubility in water relative to its production rate (Stellato et al., 2013). Since it would be equally enriched in fresh or saline groundwater (Mulligan and Charette, 2006; Sadat-Noori et al., 2015), it is considered a tracer of total groundwater discharge. However, in the sampling completed for this work, there are differences in Rn activity among the three discharge zones based on EC. These may be explained by differences in the residence time of groundwater. Similar to Ra isotopes, ^{222}Rn accumulates over time according to its half-life, requiring approximately three weeks to approach equilibrium with ^{226}Ra. In this case, ^{222}Rn is highest in fresh discharge, intermediate in the interface, and lowest in the saline discharge zone. Fresh discharge should have long (months to decades) residence times. Discharge in the interface should be a mix of density-driven brackish groundwater with a long (weeks to decades) residence time and short-flowpath saline benthic exchange that reflects a shorter-term process (hours to days). In addition, Ra adsorption to sediments is greater under freshwater conditions than under saltwater conditions, and

this likely leads to higher ^{222}Rn production in freshwater aquifers than in more saline aquifers where the Ra tends to be desorbed and flushed out.

Implications for Endmembers

Based on this conceptualization, the use of ^{222}Rn as a total SGD tracer and Ra as primarily a saline SGD tracer can present issues for the definition of the endmember. Since both Ra and Rn accumulate in groundwater over time and therefore vary in groundwater with different flowpaths, concentrations in discharging groundwater cannot be adequately represented by a single endmember value, even if a range corresponding to uncertainty is included. Rather, the discharging groundwater represents a continuum of endmembers, and the best way to capture its characteristics may be a discharge-rate weighted average. For example, using our Rn and seepage meter data, the arithmetic mean of water fluxes and ^{222}Rn activity was calculated for the first (nearest shore) and last row (most distant from shore). The ^{222}Rn activity decreased from 94.5 to 23.2 pCi/L when moving offshore, almost a factor of 4, while the flow was reduced only to half from 38.4 cm/d to 17.8 cm/d. Thus, the application of ^{222}Rn activity for the quantification of fluxes in the bay would lead to an underestimation of SGD rate. There could also be differences in endmember activities of different types of groundwater if there are heterogeneities in the abundances of parent isotopes and other aquifer characteristics that control inputs of Ra isotopes and Rn to the water.

For the correct definition of endmembers, if one component is not dominant in terms of tracer contribution, it is necessary to know *a priori* the proportion of groundwater discharge contributed by each component of discharge. The results presented in this study show that Ra isotope ratios can reflect the dominant flow mechanisms, aiding in sample classification and quantification of fluxes. Alternatively, they can be a tool for the definition of the hydrogeological conditions. For

example, Ra activity ratios can aid in the study of nutrient discharge to coastal areas and contaminant processes because the origin and circulation path of groundwater would be indicators of potential biochemical processes in each zone.

Field sampling implications

The mixing of different water types in coastal areas and the necessity of a sufficient volume of sample for measuring Ra can hinder the detection of the patterns presented to locate the different type of hydrogeological processes affecting to Ra and Rn.

As our data set demonstrates, the saltwater-freshwater interface is a diffuse boundary that can be highly irregular due to heterogeneity in aquifer hydraulic properties. This interface can be difficult to detect by direct measurements unless an extensive 2D monitoring network is used as in this experiment. A strategy for the optimization of sampling would be the use of small and surficial geophysical surveys to determine the predominance of different types of water (i.e. Kinnear et al., 2013). The measurement of salinity is highly recommended not only for sampling but also for the construction of conceptual models of freshwater-saltwater discharge (Duque et al., 2018; Michael et al., 2005) to help in the interpretation of the data collected and assess the relevance or the impact assigned to each sample.

The use of cluster sampling with several samples in small areas instead of a unique sample can help to provide an estimate of variability and uncertainty due to the natural spatial variability of the systems without excessively increasing the analytical and field work. In the case of sampling including seasonal variation, the changes in the hydrogeological conditions (i.e. water table) can lead to modifications of the saltwater-freshwater interface, affecting both endmembers in wells and measurements in discharge areas. The different flow paths and hydrogeological processes

taking place in coastal areas play an important role in the activities of radioactive tracers. Characterizing them requires additional field measurements, but this effort would be worthwhile because it would substantially reduce misinterpretations and erroneous estimates of SGD. So far, this is the first study to directly measure the spatial distribution of radioactive tracers in discharging groundwater and compare it to that in nearby wells. We think that this type of work should be more frequent in the application of these tracers instead of an anomaly.

Conclusions

Ra activity in coastal groundwater is highly variable due to the salinity differences within the saltwater-freshwater interface. Even over short distances such as those presented in this study and under apparent homogeneous hydrogeological conditions and sedimentary composition, considerable spatial variability occurs.

Ra activity is affected by the hydrogeological processes taking place in coastal areas. The freshwater zone is defined by the lower salinity and lower Ra activity, the interface zone presents higher activities in ^{226}Ra and ^{228}Ra due to the longer flow path as a consequence of density driven flow, and higher activities of ^{223}Ra and ^{224}Ra are measured in the zones dominated by recirculation of saline water. Applying ^{222}Rn as a total SGD tracer can be problematic when short-term circulation patterns dominate the hydrological conditions, because this type of circulation was associated with lower Rn activity in groundwater. The results presented in this work showed a higher ^{222}Rn activity in the areas dominated by freshwater due to the longer groundwater residence time in the aquifer and greater concentration of adsorbed Ra on aquifer surfaces.

The use of seepage meters for sampling submarine groundwater discharge has several advantages. Used in clusters, measurement can be a useful alternative for the definition of spatially variable endmembers and can enable better assessment of uncertainty. Our results indicate that a grid of seepage meters provides a more accurate characterization of the discharging groundwater endmember compared with wells. The use of inland wells as groundwater endmembers can introduce potentially large errors, since various processes that affect natural tracer concentrations can take place along the flow path between the well location and the coastal discharge area. The main challenge in using seepage meters is the restrictions associated with installation and the amount of manual labor required.

While radium and radon isotopes are useful tools, as demonstrated in multiple SGD studies, they must be used carefully. The very large impacts of the origin and flowpaths of discharging groundwater on tracer concentrations should be a major consideration in their application because it can reduce their reliability or even render them useless as indicators of hydrologic processes. Moving forward, the community must recognize these dependencies and make every effort to apply radiochemical tracers in the most accurate way possible, even if that means making more measurements, conducting uncertainty analyses, and collaborating across disciplines. Taking into consideration the hydrogeological conditions (saltwater-freshwater interface, seasonal changes, residence times, the design of sampling surveys considering the discharge conceptual models and the natural spatial variability) will lead to more accurate results in the estimation of submarine groundwater discharge.

Acknowledgments

We thank Thomas W. Brooks, Riley Brown, Graham Prowse, Rachel Owrutsky, Michael Shand and Raquel Freitas for field and laboratory assistance. The research leading to these results has received funding from the European Union Seventh Framework Programme [FP7/2007-2013] under grant agreement number [624496]. It has also received funding from the US National Science Foundation: NSF EAR-1151733 to HM, the Brazil Scientific Mobility Program (to support undergraduate research by Raquel Freitas in KLK's lab) and the U.S. Agency for International Development (for support of a postdoctoral scholarship for Usama Abu Risha in NCS's lab). This work was carried out as part of the activities of the Aarhus University Centre for Water Technology, WATEC.

References

Andres, A.S., 1992. Estimate of nitrate flux to Rehoboth and Indian River Bays, Delaware through direct discharge of ground water. Open File Rep. 35. Delaware Geol. Surv. Newark, 36.

Andres, S.A., Michael, H., Rusoniello, C.R., Fernandez, C., He, C., Madsen, J.A., 2015. Investigation of submarine groundwater discharge at Holts Landing State Park: Hydrogeologic framework, groundwater level and salinity observations. Rep. Investig. No. 80 38.

Atkins, M.L., Santos, I.R., Ruiz-Halpern, S., Maher, D.T., 2013. Carbon dioxide dynamics driven by groundwater discharge in a coastal floodplain creek. J. Hydrol. 493, 30–42. https://doi.org/10.1016/j.jhydrol.2013.04.008

Bratton, J.F., Böhlke, J.K., Manheim, F.T., Krantz, D.E., 2004. Ground water beneath coastal bays of the delmarva peninsula: Ages and nutrients. Ground Water 42, 1021–1034. https://doi.org/10.1111/j.1745-6584.2004.tb02641.x

Burnett, W.C., Aggarwal, P.K., Aureli, A., Bokuniewicz, H., Cable, J.E., Charette, M.A., Kontar, E., Krupa, S., Kulkarni, K.M., Loveless, A., Moore, W.S., Oberdorfer, J.A., Oliveira, J., Ozyurt, N., Povinec, P., Privitera, A.M.G., Rajar, R., Ramessur, R.T., Scholten, J., Stieglitz, T., Taniguchi, M., Turner, J. V., 2006. Quantifying submarine groundwater discharge in the coastal zone via multiple methods. Sci. Total Environ. 367, 498–543. https://doi.org/10.1016/j.scitotenv.2006.05.009

Burnett, W.C., Dulaiova, H., 2003. Estimating the dynamics of groundwater input into the

coastal zone via continuous radon-222 measurements. J. Environ. Radioact. 69, 21–35. https://doi.org/10.1016/S0265-931X(03)00084-5

Burnett, W.C., Peterson, R.N., Santos, I.R., Hicks, R.W., 2010. Use of automated radon measurements for rapid assessment of groundwater flow into Florida streams. J. Hydrol. 380, 298–304. https://doi.org/10.1016/j.jhydrol.2009.11.005

Cable, J.E., Burnett ', W.C., Chanton, J.P., Weatherly, G.L., 1996. Estimating groundwater discharge into the northeastern Gulf of Mexico using radon-222. EPSL ELSEVIER Earth Planet. Sci. Lett. 144, 591–604.

Cerdà-domènech, M., Rodellas, V., Folch, A., Garcia-orellana, J., 2017. Science of the Total Environment Constraining the temporal variations of Ra isotopes and Rn in the groundwater end-member : Implications for derived SGD estimates. Sci. Total Environ. 595, 849–857. https://doi.org/10.1016/j.scitotenv.2017.03.005

Charette, M.A., 2007. Hydrologic forcing of submarine groundwater discharge: Insight from a seasonal study of radium isotopes in a groundwater-dominated salt marsh estuary. Limnol. Oceanogr. 52, 230–239. https://doi.org/10.4319/lo.2007.52.1.0230

Charette, M.A., Buesseler, K.O., Andrews, J.E., 2001. Utility of radium isotopes for evaluating the input and transport of groundwater-derived nitrogen to a Cape Cod estuary. Limnol. Oceanogr. 46, 465–470. https://doi.org/10.4319/lo.2001.46.2.0465

Cho, H.M., Kim, G., 2016. Determining groundwater Ra end-member values for the estimation of the magnitude of submarine groundwater discharge using Ra isotope tracers. Geophys. Res. Lett. 43, 3865–3871. https://doi.org/10.1002/2016GL068805

Chrzastowski, M.J., 1986. Stratigraphy and geologic history of a Holocene lagoon Rehoboth Bay and Indian River Bay, Delaware. University of Delaware, Newark, Delaware.

Corbett, D., Chanton, J., Burnett, W., Dillon, K., Rutkowski, C., Fourqurean, J., 1999. Patterns of groundwater discharge into Florida Bay. Limnol. Oceanogr. 44, 1045–1055. https://doi.org/10.4319/lo.1999.44.4.1045

Dimova, N.T., Burnett, W.C., Chanton, J.P., Corbett, J.E., 2013. Application of radon-222 to investigate groundwater discharge into small shallow lakes. J. Hydrol. 486, 112–122. https://doi.org/10.1016/j.jhydrol.2013.01.043

Dragović, S.D., Janković-Mandić, L.J., Dragović, R.M., Dordević, M.M., Dokić, M.M., 2012. Spatial distribution of the226Ra activity concentrations in well and spring waters in Serbia and their relation to geological formations. J. Geochemical Explor. 112, 206–211. https://doi.org/10.1016/j.gexplo.2011.08.013

Dulaiova, H., Burnett, W.C., 2004. An efficient method for γ -spectrometric determination of radium-226 , 228 via manganese fibers. Limnol. Oceanogr. Methods 2, 256–261. https://doi.org/10.4319/lom.2004.2.256

Dulaiova, H., Gonneea, M.E., Henderson, P.B., Charette, M.A., 2008. Geochemical and physical sources of radon variation in a subterranean estuary — Implications for groundwater radon activities in submarine groundwater discharge studies 110, 120–127. https://doi.org/10.1016/j.marchem.2008.02.011

Duque, C., Gómez Fontalva, J.M., Murillo Díaz, J.M., Calvache, M.L., 2018. Estimating the water budget in a semi-arid region (Torrevieja aquifer—south-east Spain) by assessing groundwater numerical models and hydrochemical data. Environ. Earth Sci. 77. https://doi.org/10.1007/s12665-017-7200-x

Duque, Carlos, Haider, K., Sebok, E., Sonnenborg, T.O., Engesgaard, P., 2018. A conceptual model for groundwater discharge to a coastal brackish lagoon based on seepage measurements (Ringkøbing Fjord, Denmark). Hydrol. Process. 32, 3352–3364. https://doi.org/10.1002/hyp.13264

Duque, C., Knee, K.L., Russoniello, C.J., Sherif, M., Abu Risha, U.A., Sturchio, N.C., Michael, H.A., 2019. Submarine groundwater discharge data at meter scale (^{223}Ra, ^{224}Ra, ^{226}Ra, ^{228}Ra and ^{222}Rn) in Indian River Bay (Delaware, US). Data Br.

Eissa, M.A., de Dreuzy, J.R., Parker, B., 2018. Integrative management of saltwater intrusion in poorly-constrained semi-arid coastal aquifer at Ras El-Hekma, Northwestern Coast, Egypt. Groundw. Sustain. Dev. 6, 57–70. https://doi.org/10.1016/j.gsd.2017.10.002

Ellins, K.K., Roman-Mas, A., Lee, R., 1990. Using222Rn to examine groundwater/surface discharge interaction in the Rio Grande de Manati, Puerto Rico. J. Hydrol. 115, 319–341. https://doi.org/10.1016/0022-1694(90)90212-G

Elsinger, R.J., Moore, W.S., 1984. 226Ra and 228Ra in the mixing zones of the Pee Dee River-Winyah Bay, Yangtze River and Delaware Bay Estuaries. Estuar. Coast. Shelf Sci. 18, 601–613. https://doi.org/10.1016/0272-7714(84)90033-7

Gallardo, A.H., 2019. Hydrogeological characterisation and groundwater exploration for the development of irrigated agriculture in the West Kimberley region, Western Australia. Groundw. Sustain. Dev. 8, 187–197. https://doi.org/10.1016/j.gsd.2018.11.004

Garcia-Solsona, E., Masqué, P., Garcia-Orellana, J., Rapaglia, J., Beck, A.J., Cochran, J.K., Bokuniewicz, H.J., Zaggia, L., Collavini, F., 2008. Estimating submarine groundwater discharge around Isola La Cura, northern Venice Lagoon (Italy), by using the radium quartet. Mar. Chem. 109, 292–306. https://doi.org/10.1016/j.marchem.2008.02.007

Girault, F., Perrier, F., Przylibski, T.A., 2016. Radon-222 and radium-226 occurrence in water: a review. Geol. Soc. London, Spec. Publ. 451, SP451.3. https://doi.org/10.1144/SP451.3

Gonneea, M.E., Morris, P.J., Dulaiova, H., Charette, M.A., 2008. New perspectives on radium behavior within a subterranean estuary. Mar. Chem. 109, 250–267. https://doi.org/10.1016/j.marchem.2007.12.002

Heiss, J.W., Michael, H.A., 2014. Saltwater-freshwater mixing dynamics in a sandy beach aquifer over tidal, spring-neap, and seasonal cycles. Water Resour. Res. 50, 6747–6766. https://doi.org/10.1002/2014WR015574.Received

Hughes, A.L.H., Wilson, A.M., Moore, W.S., 2015. Groundwater transport and radium variability in coastal porewaters. Estuar. Coast. Shelf Sci. 164, 94–104. https://doi.org/10.1016/j.ecss.2015.06.005

Johannes, R.E., 1980. The ecological significance of submarine discharge of groundwater.pdf. Mar. Ecol. 3, 365–373.

Kelly, R.P., Moran, S.B., 2002. Seasonal changes in groundwater input to a well-mixed estuary estimated using radium isotopes and implications for coastal nutrient budgets. Limnol. Oceanogr. 47, 1796–1807. https://doi.org/10.4319/lo.2002.47.6.1796

Kim, G., Burnett, W.C., Dulaiova, H., Swarzenski, P.W., Moore, W.S., 2001. Measurement of ^{224}Ra and ^{226}Ra Activities in Natural Waters Using a Radon-in-Air Monitor. Environ. Sci. Technol. 35, 4680–4683. https://doi.org/10.1021/es010804u

Kim, G., Ryu, J.W., Yang, H.S., Yun, S.T., 2005. Submarine groundwater discharge (SGD) into the Yellow Sea revealed by228Ra and226Ra isotopes: Implications for global silicate fluxes. Earth Planet. Sci. Lett. 237, 156–166. https://doi.org/10.1016/j.epsl.2005.06.011

Kinnear, J.A., Binley, A., Duque, C., Engesgaard, P.K., 2013. Using geophysics to map areas of potential groundwater discharge into Ringkøbing Fjord, Denmark. Lead. Edge 32. https://doi.org/10.1190/tle32070792.1

Knee, K.L., Layton, B.A., Street, J.H., Boehm, A.B., Paytan, A., 2008. Sources of nutrients and fecal indicator bacteria to nearshore waters on the north shore of Kaua'i (Hawai'i, USA). Estuaries and Coasts 31, 607–622. https://doi.org/10.1007/s12237-008-9055-6

Kohout, F.A., 1964. The flow of fresh water and salt water in the Biscayne Aquifer of the Miami area, Florida. 161G-C 12–32.

Krantz, D.E., Manheim, F.T., Bratton, J.F., Phelan, D.J., 2004. Hydrogeologic setting and ground water flow beneath a section of Indian River Bay, Delaware. Ground Water 42, 1035–1051. https://doi.org/10.1111/j.1745-6584.2004.tb02642.x

Krest, J.M., Harvey, J.W., 2003. Using natural distributions of short-lived radium isotopes to quantify groundwater discharge and recharge. Limnol. Oceanogr. 48, 290–298. https://doi.org/10.4319/lo.2003.48.1.0290

Krest, J.M., Moore, W.S., Gardner, L.R., Morris, J.T., 2000. Marsh nutrient export supplied by groundwater discharge: Evidence from radium measurements. Global Biogeochem. Cycles 14, 167–176. https://doi.org/10.1029/1999GB001197

Lauria, D.C., Almeida, R.M.R., Sracek, O., 2004. Behavior of radium, thorium and uranium in groundwater near the Buena Lagoon in the Coastal Zone of the State of Rio de Janeiro, Brazil. Environ. Geol. 47, 11–19. https://doi.org/10.1007/s00254-004-1121-1

Liu, Y., Jiao, J.J., Liang, W., Luo, X., 2018. Using Tidal Fluctuation-Induced Dynamics of Radium Isotopes (224Ra, 223Ra, and 228Ra) to Trace the Hydrodynamics and Geochemical Reactions in a Coastal Groundwater Mixing Zone. Water Resour. Res. 54, 2909–2930. https://doi.org/10.1002/2017WR022456

Makings, U., Santos, I.R., Maher, D.T., Golsby-Smith, L., Eyre, B.D., 2014. Importance of budgets for estimating the input of groundwater-derived nutrients to an eutrophic tidal river and estuary. Estuar. Coast. Shelf Sci. 143, 65–76. https://doi.org/10.1016/j.ecss.2014.02.003

Michael, H. a, Mulligan, A.E., Harvey, C.F., 2005. Seasonal oscillations in water exchange between aquifers and the coastal ocean. Nature 436, 1145–1148. https://doi.org/10.1038/nature03935

Michael, H.A., Charette, M.A., Harvey, C.F., 2011. Patterns and variability of groundwater flow and radium activity at the coast: A case study from Waquoit Bay, Massachusetts. Mar. Chem. 127, 100–114. https://doi.org/10.1016/j.marchem.2011.08.001

Michael, H.A., Lubetsky, J.S., Harvey, C.F., 2003. Characterizing submarine groundwater discharge: A seepage meter study in Waquoit Bay, Massachusetts. Geophys. Res. Lett. 30. https://doi.org/10.1029/2002GL016000

Milliman, J.D., 1993. Production and accumulation of calcium carbonate in the ocean: Budget of a nonsteady state. Global Biogeochem. Cycles 7, 927–957. https://doi.org/10.1029/93GB02524

Mook, W.E., 2001. Environmental Isotopes in the hydrological cycle. Principles and applications. Theory, Methods, Rev. IHP-V Tech. Doc. Hydrol. UNESCO – IAEA 1.

Moore, W.S., 2008. Fifteen years experience in measuring224Ra and223Ra by delayed-coincidence counting. Mar. Chem. 109, 188–197. https://doi.org/10.1016/j.marchem.2007.06.015

Moore, W.S., 2003. Sources and fluxes of submarine groundwater discharge delineated by radium isotopes. Biogeochemistry 66, 75–93. https://doi.org/10.1023/B:BIOG.0000006065.77764.a0

Moore, W.S., 1996. Large groundwater inputs to coastal waters revealed by 226Ra enrichments. Nature. https://doi.org/10.1038/380612a0

Moore, W.S., 1976. Sampling 228Ra in the deep ocean 23, 647–651.

Moore, W.S., Arnold, R., 1996. Measurement of Ra and Ra in coastal waters using a delayed coincidence counter. J. Geophys. Res. Ocean. 101, 1321–1329. https://doi.org/10.1029/95JC03139

Moore, W.S., Reid, D.F., 1973. Extraction of radium from natural waters using manganese-impregnated acrylic fibers. J. Geophys. Res. 78, 8880–8886.

Mulligan, A.E., Charette, M.A., 2006. Intercomparison of submarine groundwater discharge estimates from a sandy unconfined aquifer. J. Hydrol. 327, 411–425. https://doi.org/10.1016/j.jhydrol.2005.11.056

Murdoch, L.C., Kelly, S.E., 2003. Factors affecting the performance of conventional seepage meters. Water Resour. Res. 39. https://doi.org/10.1029/2002WR001347

NOAA/NCDC, 2010. Time bias corrected divisional temperature-precipitation-drought index (TD-9640). Natl. Ocean. Atmos. Adm. (NOAA)/National Climactic Data Cent.

Onishchenko, A., Zhukovsky, M., Veselinovic, N., Zunic, Z.S., 2010. Radium-226 concentration in spring water sampled in high radon regions. Appl. Radiat. Isot. 68, 825–827. https://doi.org/10.1016/j.apradiso.2009.09.050

Peterson, R.N., Santos, I.R., Burnett, W.C., 2010. Evaluating groundwater discharge to tidal rivers based on a Rn-222 time-series approach. Estuar. Coast. Shelf Sci. 86, 165–178. https://doi.org/10.1016/j.ecss.2009.10.022

Rama, Moore, W.S., 1996. Using the radium quartet for evaluating groundwater input and water exchange in salt marshes. Geochim. Cosmochim. Acta 60, 4645–4652.

Rapaglia, J., Di Sipio, E., Bokuniewicz, H., Maria Zuppi, G., Zaggia, L., Galgaro, A., Beck, A., 2010. Groundwater connections under a barrier beach: A case study in the Venice Lagoon. Cont. Shelf Res. 30, 119–126. https://doi.org/10.1016/j.csr.2009.10.001

Robinson, C., Li, L., Prommer, H., 2007. Tide-induced recirculation across the aquifer-ocean interface. Water Resour. Res. 43, 1–14. https://doi.org/10.1029/2006WR005679

Rosenberry, D.O., 2005. Integrating seepage heterogeneity with the use of ganged. Limnol. Oceanogr. Methods 3, 131–142.

Russoniello, C.J., Fernandez, C., Bratton, J.F., Banaszak, J.F., Krantz, D.E., Andres, A.S., Konikow, L.F., Michael, H.A., 2013. Geologic effects on groundwater salinity and discharge into an estuary. J. Hydrol. 498, 1–12. https://doi.org/10.1016/j.jhydrol.2013.05.049

Russoniello, C.J., Heiss, J.W., Michael, H.A., 2018. Variability in Benthic Exchange Rate, Depth, and Residence Time Beneath a Shallow Coastal Estuary. J. Geophys. Res. Ocean. 123, 1860–1876. https://doi.org/10.1002/2017JC013568

Russoniello, C.J., Konikow, L.F., Kroeger, K.D., Fernandez, C., Andres, A.S., Michael, H.A., 2016. Hydrogeologic controls on groundwater discharge and nitrogen loads in a coastal watershed. J. Hydrol. 538, 783–793. https://doi.org/10.1016/j.jhydrol.2016.05.013

Russoniello, C.J., Michael, H.A., 2015. Investigation of Seepage Meter Measurements in Steady Flow and Wave Conditions. Groundwater 53, 959–966. https://doi.org/10.1111/gwat.12302

Sadat-Noori, M., Santos, I.R., Sanders, C.J., Sanders, L.M., Maher, D.T., 2015. Groundwater discharge into an estuary using spatially distributed radon time series and radium isotopes. J. Hydrol. 528, 703–719. https://doi.org/10.1016/j.jhydrol.2015.06.056

Sadat-Noori, M., Santos, I.R., Tait, D.R., Maher, D.T., 2016. Fresh meteoric versus recirculated saline groundwater nutrient inputs into a subtropical estuary. Sci. Total Environ. 566–567, 1440–1453. https://doi.org/10.1016/j.scitotenv.2016.06.008

Sanchez, F., Rodriguez-Alvarez, M.J., 1999. Effect of pH, temperature, conductivity and sediment size on thorium and radium activities along Jucar River (Spain). J. Radioanal. Nucl. Chem. 242, 671–681. https://doi.org/10.1007/BF02347378

Santos, I.R., Bryan, K.R., Pilditch, C.A., Tait, D.R., 2014. Influence of porewater exchange on nutrient dynamics in two New Zealand estuarine intertidal flats. Mar. Chem. 167, 57–70. https://doi.org/10.1016/j.marchem.2014.04.006

Santos, I.R., Eyre, B.D., Huettel, M., 2012. The driving forces of porewater and groundwater flow in permeable coastal sediments: A review. Estuar. Coast. Shelf Sci. 98, 1–15. https://doi.org/10.1016/j.ecss.2011.10.024

Sawyer, A.H., Lazareva, O., Kroeger, K.D., Crespo, K., Chan, C.S., Stieglitz, T., Michael, H. a., 2014. Stratigraphic controls on fluid and solute fluxes across the sediment-water interface of an estuary. Limnol. Oceanogr. 59, 997–1010. https://doi.org/10.4319/lo.2014.59.3.0997

Sawyer, A.H., Shi, F., Kirby, J.T., Michael, H.A., 2013. Dynamic response of surface water-groundwater exchange to currents, tides, and waves in a shallow estuary. J. Geophys. Res. Ocean. 118, 1749–1758. https://doi.org/10.1002/jgrc.20154

Schmidt, A., Stringer, C.E., Haferkorn, U., Schubert, M., 2009. Quantification of groundwater discharge into lakes using radon-222 as naturally occurring tracer. Environ. Geol. 56, 855–863. https://doi.org/10.1007/s00254-008-1186-3

Schubert, M., Paschke, A., Lieberman, E., Burnett, W.C., 2012. Air-water partitioning of 222Rn and its dependence on water temperature and salinity. Environ. Sci. Technol. 46, 3905–3911. https://doi.org/10.1021/es204680n

Shaw, R.D., Prepas, E.. E.., 1989. Anomalous , Short-Term Influx of Water Into Seepage Meters. Limnol. Oceanogr. 34, 1343–1351.

Smith, C.G., Cable, J.E., Martin, J.B., Roy, M., 2008. Evaluating the source and seasonality of submarine groundwater discharge using a radon-222 pore water transport model. Earth Planet. Sci. Lett. 273, 312–322. https://doi.org/10.1016/j.epsl.2008.06.043

Stachelhaus, S.L., Moran, S.B., Kelly, R.P., 2012. An evaluation of the efficacy of radium isotopes as tracers of submarine groundwater discharge to southern Rhode Island's coastal ponds. Mar. Chem. 130–131, 49–61. https://doi.org/10.1016/j.marchem.2012.01.001

Stellato, L., Terrasi, F., Marzaioli, F., Belli, M., Sansone, U., Celico, F., 2013. Is 222Rn a suitable tracer of stream-groundwater interactions? A case study in central Italy. Appl. Geochemistry 32, 108–117. https://doi.org/10.1016/j.apgeochem.2012.08.022

Stieglitz, T., Rapaglia, J., Bokuniewicz, H., 2008. Estimation of submarine groundwater discharge from bulk ground electrical conductivity measurements. J. Geophys. Res. Ocean. 113, 1–15. https://doi.org/10.1029/2007JC004499

Street, J.H., Knee, K.L., Grossman, E.E., Paytan, A., 2008. Submarine groundwater discharge and nutrient addition to the coastal zone and coral reefs of leeward Hawai'i. Mar. Chem. 109, 355–376. https://doi.org/10.1016/j.marchem.2007.08.009

Sturchio, N.C., Banner, J.L., Binz, C.M., Heraty, L.B., Musgrove, M., 2001. Radium geochemistry of ground waters in Paleozoic carbonate aquifers, midcontinent, USA. Appl. Geochemistry 16, 109–122. https://doi.org/10.1016/S0883-2927(00)00014-7

Sun, Y., Torgersen, T., 1998. Rapid and precise measurement method for adsorbed 224 Ra on sediments. Mar. Chem. 61, 163–171.

Swarzenski, P.W., 2007. U/Th series radionuclides as coastal groundwater tracers. Chem. Rev. 107, 663–674. https://doi.org/10.1021/cr0503761

Tamborski, J.J., Cochran, J.K., Bokuniewicz, H.J., 2017. Application of 224Ra and 222Rn for evaluating seawater residence times in a tidal subterranean estuary. Mar. Chem. 189, 32–45. https://doi.org/10.1016/j.marchem.2016.12.006

Tréguer, P.J., De La Rocha, C.L., 2013. The World Ocean Silica Cycle. Ann. Rev. Mar. Sci. 5, 477–501. https://doi.org/10.1146/annurev-marine-121211-172346

Valiela, I., Costa, J., Foreman, K., Teal, J.M., Howes, B., Biogeochemistry, S., Inputs, G., Aug, W., Valiela, I., Costa, J., Foreman, K., Teal, J.M., Howes, B., Aubrey, D., 1990. Transport of Groundwater-Borne Nutrients from Watersheds and Their Effects on Coastal Waters. Biogeochemistry 10, 177–197.

Vinson, D.S., Vengosh, A., Hirschfeld, D., Dwyer, G.S., 2009. Relationships between radium and radon occurrence and hydrochemistry in fresh groundwater from fractured crystalline rocks, North Carolina (USA). Chem. Geol. 260, 159–171. https://doi.org/10.1016/j.chemgeo.2008.10.022

Xin, P., Robinson, C., Li, L., Barry, D.A., Bakhtyar R., 2010. Effects of wave forcing on a subterranean estuary. Water Resour. Res. 46.

Zhuo, W.H., Iida, T., Yang, X.T., 2001. Occurrence of Rn-222, Ra-226, Ra-228 and U in groundwater in Fujian Province, China. J. Environ. Radioact. 53, 111–120. https://doi.org/10.1016/s0265-931x(00)00108-9

Figure captions

Figure 1. Conceptualization of flowpaths and corresponding SGD over the map of interpolated EC measured with groundwater samplers (vertical section) and seepage meters (horizontal bayfloor). 1) Freshwater flow, 2) density-driven convection, and 3) benthic exchange. Blue refers to freshwater, and red to saltwater (color scale can be found in figure 3).

Figure 2. Location of the study area and distribution of field measurements and wells in Holts Landing State Park. Seepage meter locations and numbers are shown in monitoring area inset

Figure 3. A) Interpolation of electrical conductivity, B) interpolation of fluxes, C) flux vs EC in seepage meters. Sampling point locations are shown in A and B, and colored by discharge zone category

Figure 4. Comparison of ^{222}Rn, ^{223}Ra, ^{224}Ra, ^{226}Ra and ^{228}Ra in discharging groundwater for each discharge zone (median, range maximum and minimum and outliers are presented)

Figure 5. Spatial distribution of ^{228}Ra, ^{226}Ra, ^{223}Ra and ^{224}Ra activities in discharging groundwater. The colors of the dots correspond with freshwater (blue), interface water (yellow) and saltwater (red)

Figure 6. (Left) ^{228}Ra and (Right) ^{222}Rn activity (dpm/100 L) vs electrical conductivity (mS/cm) of groundwater collected in seepage meter locations (circles), well 4 (blue diamonds) and baywater (red squares). Error bars correspond to analytical error. For ^{222}Rn, data for samples collected in well 4 at different times in preliminary surveys (October 2015, December 2015) are also shown.

Figure 7. Ratios of Ra isotopes (size of the dots is proportional to the value in white) and electrical conductivity distribution map (colors). The freshwater zone ratios have been excluded due to erratic values when dividing by near-zero denominators).

Table captions

Table 1. Number of samples (n), arithmetic mean (μ), maximum (Max), minimum (Min), and standard deviation (S.D.) of flow measured with seepage meters and ^{222}Rn activity measurements with analytical errors for the categories established based on EC.

Table 2. Arithmetic mean, maximum, minimum, and standard deviation of Ra isotope activity measurements with analytical errors.

Table 3. Universal Transverse Mercator (UTM) coordinates, ^{223}Ra, ^{224}Ra, ^{226}Ra, ^{228}Ra, ^{222}Rn activities with analytical error, volume of sample (V) and EC of the wells.

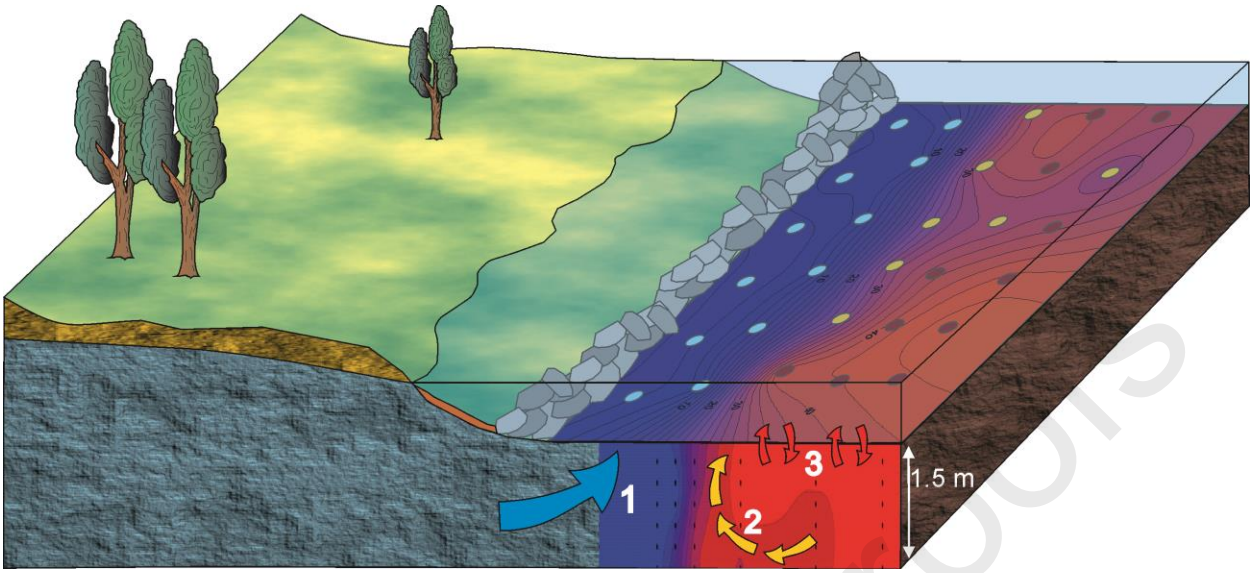

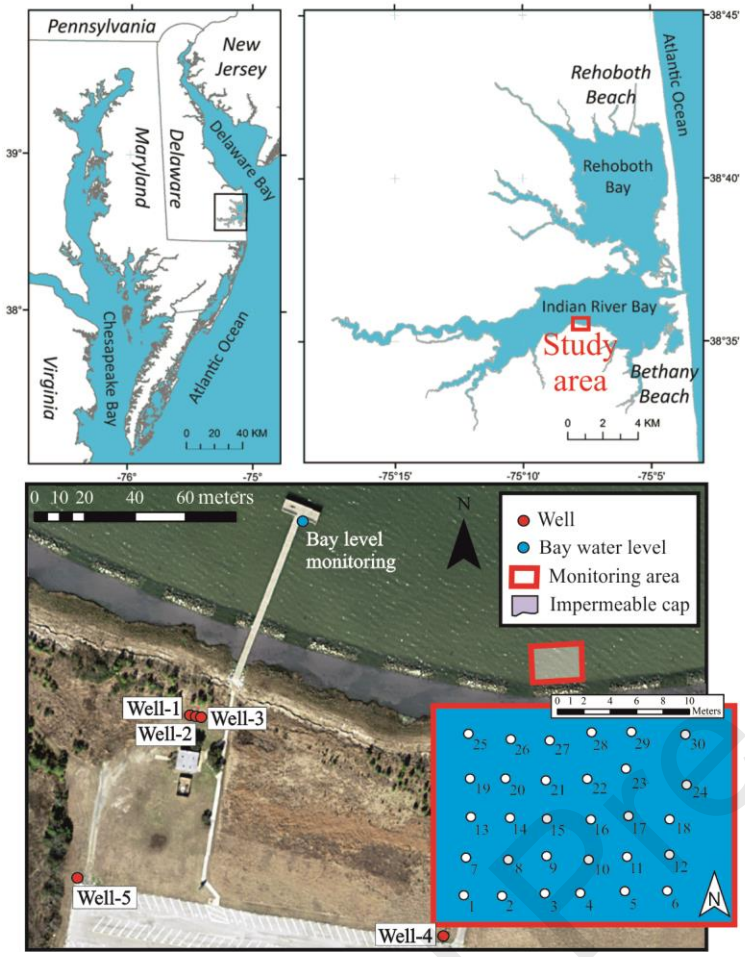

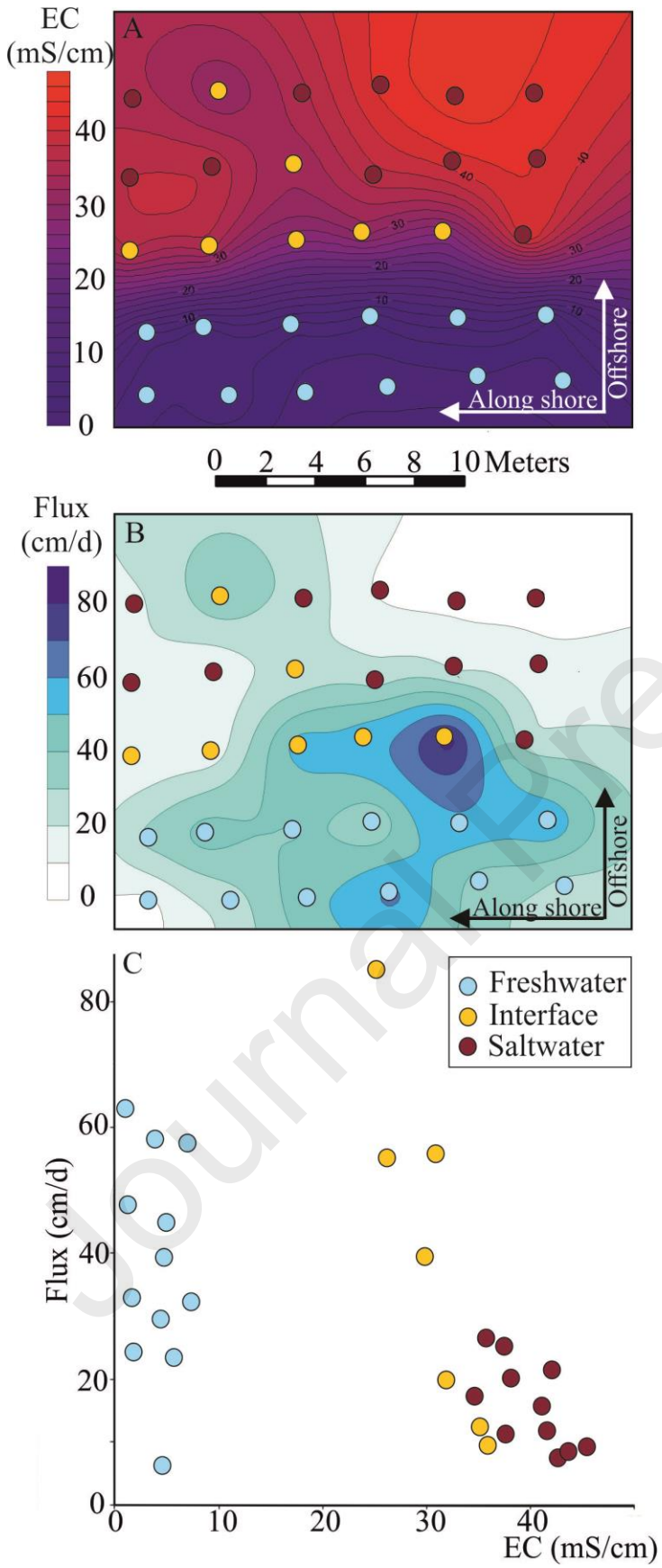

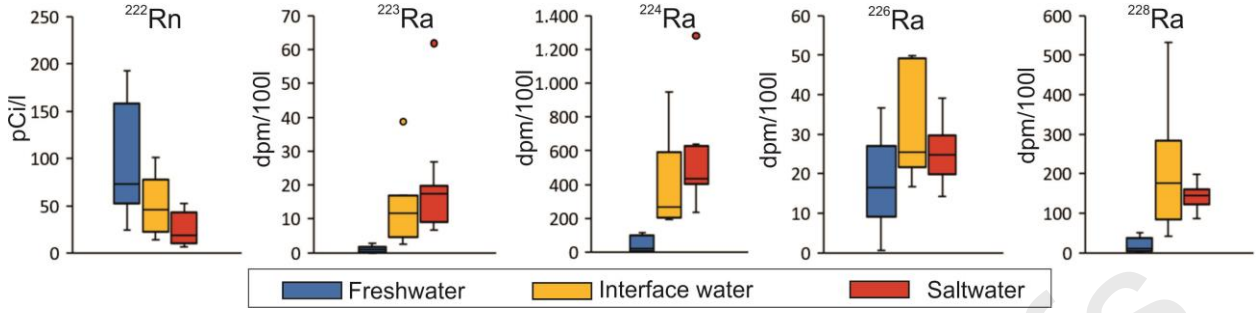

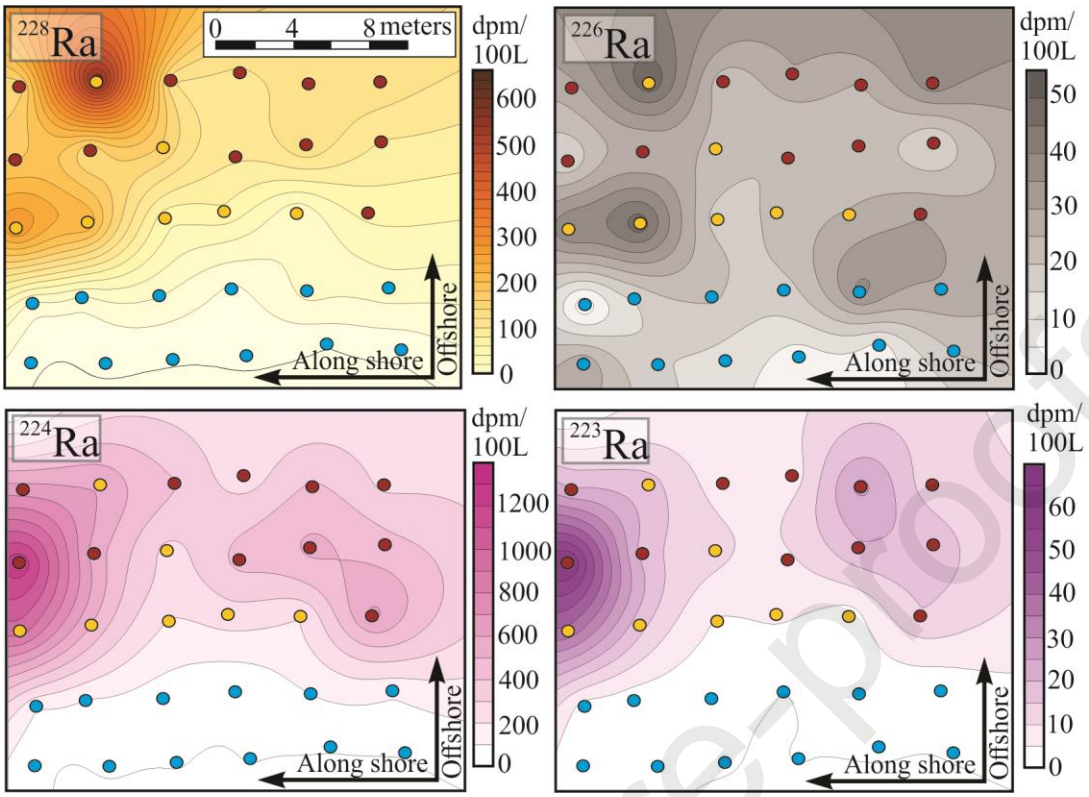

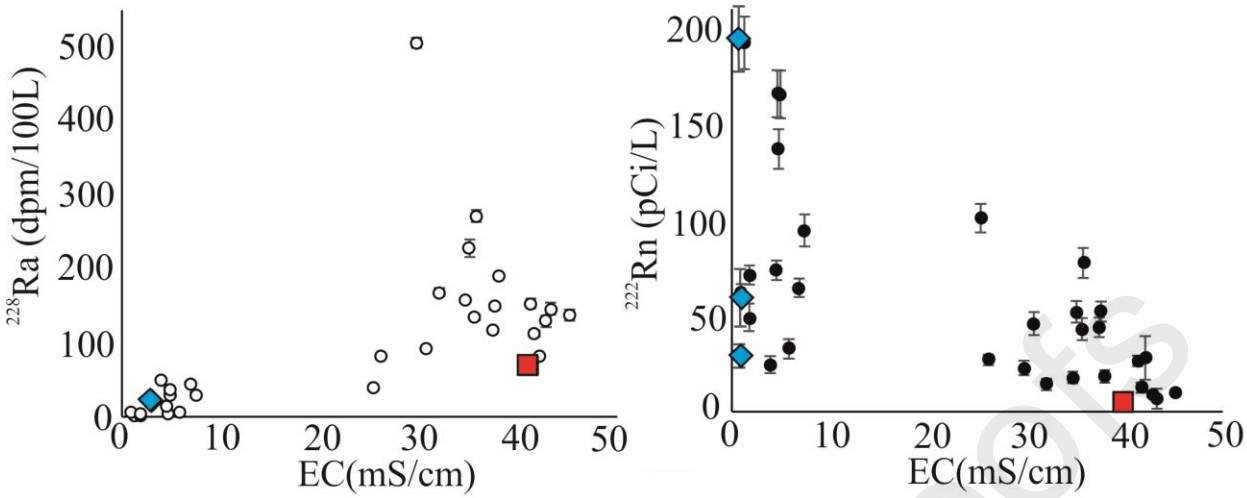

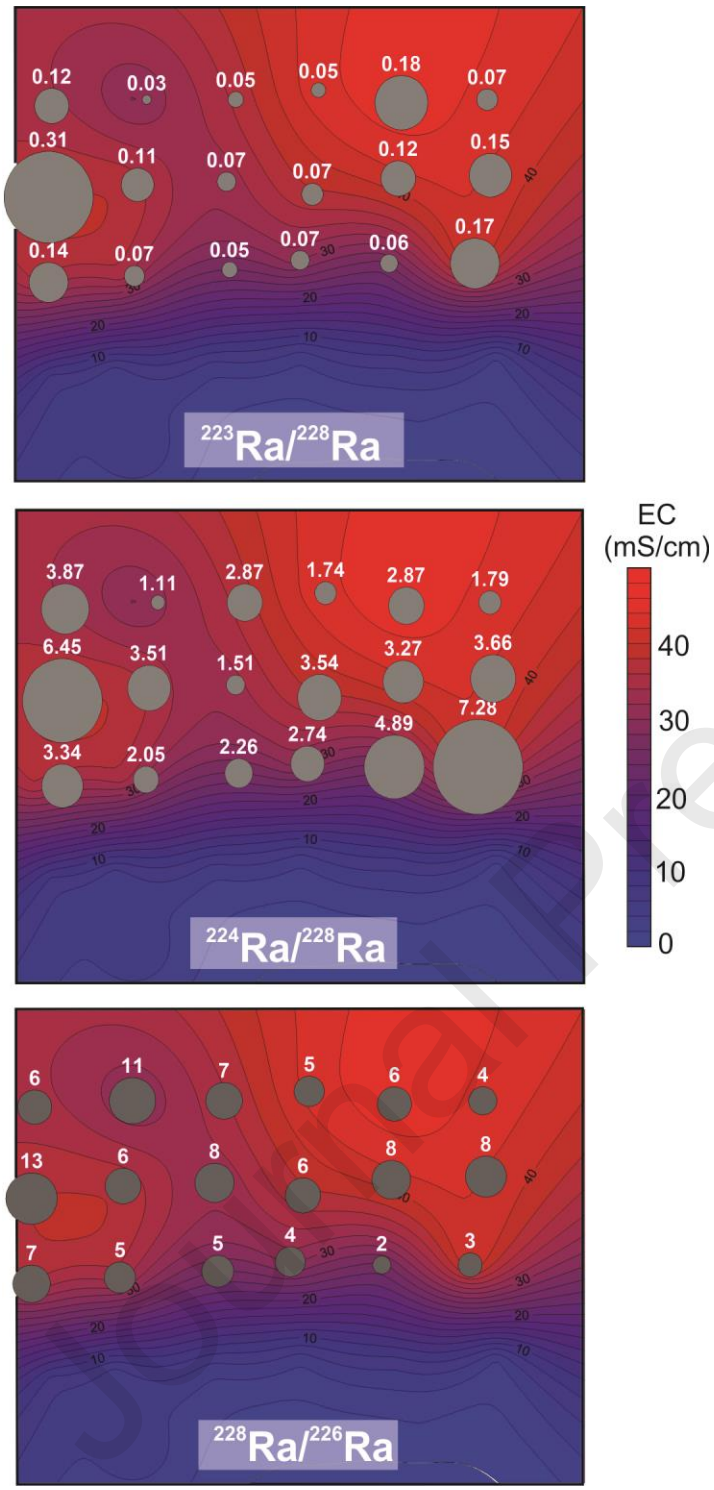

Table 1

	Flow (cm/d)					^{222}Rn (pCi/L)				
	n	μ	Max	Min	S.D.	n	μ	Max	Min	S.D.
All data	30	30	85	6	20	30	58±6	192±14	7±5	50±3
Freshwater	12	38	63	6	17	12	95±12	192±14	25±4	57±4
Interface	7	40	85	10	28	7	49±5	101±7	14±3	31±2
Saltwater	11	16	26	8	7	11	24±4	52±5	7±5	16±3

Table 2

	^{226}Ra (dpm/100L)					^{228}Ra (dpm/100L)				
	n	μ	Max	Min	S.D.	n	μ	Max	Min	S.D.
All data	30	24±10	50±6	1±16	11±10	30	109±4	532±7	1±1	111±3
Freshwater	12	15±10	37±2	1±16	10±1	12	7±2	51±2	1±1	19±1
Interface	7	32±8	50±7	17±4	14±6	7	208±6	532±7	41±1	167±4
Saltwater	11	24±11	39±15	14±3	7±10	11	144±5	199±3	86±3	29±2
	^{223}Ra (dpm/100L)					^{224}Ra (dpm/100L)				
	n	μ	Max	Min	S.D.	n	μ	Max	Min	S.D.
All data	30	11±4	62±11	0±0	14±5	30	310±78	1282±529	4±2	307±113
Freshwater	12	1±1	3±1	0±0	1±0	12	12±7	117±7	4±2	46±4
Interface	7	14±5	39±17	3±1	12±6	7	423±85	951±310	193±14	277±106
Saltwater	11	19±7	62±11	7±4	15±4	11	530±152	1282±529	236±87	281±135

Table 3

Sample	UTM X	UTM Y	^{226}Ra (dpm/100L)	^{228}Ra (dpm/100L)	^{223}Ra (dpm/100L)	^{224}Ra (dpm/100L)	V (L)	^{222}Rn (pCi/L)	EC mS/cm
Well 1	488788.0	4271452.3	70±4	46±2	4±2	N.A.	39.30	17±8	5.05
Well 2	488790.4	4271451.9	104±8	136±5	8±3	325±505	41.00	25±6	1.25
Well 3	488793.0	4271451.6	149±10	897±11	141±30	3948±1192	39.10	33±20	20.12
Well 4	488888.5	4271365.8	20±6	23±3	4±1	82±14	39.30	26+6	0.6
Well 5	488746.0	4271382.3	2±12	33±3	3±1	56±10	38.80	2+0	N.A.

Hydrogeological processes in coastal areas affect to Ra and Rn activity

Sampling discharging groundwater is more accurate with seepage meters than wells

SGD estimated with Ra and Rn requires knowing origin and flowpaths of groundwater

Declaration of interests

☒ The authors declare that they have no known competing financial interests or personal relationships that could have appeared to influence the work reported in this paper.

☐The authors declare the following financial interests/personal relationships which may be considered as potential competing interests: